The American Journal of Human Genetics, Volume *111*

Supplemental information

De novo missense variants in *HDAC3* leading to epigenetic machinery dysfunction are associated with a variable neurodevelopmental disorder

Jihoon G. Yoon, Seong-Kyun Lim, Hoseok Seo, Seungbok Lee, Jaeso Cho, Soo Yeon Kim, Hyun Yong Koh, Annapurna H. Poduri, Vijayalakshmi Ramakumaran, Pradeep Vasudevan, Martijn J. de Groot, Jung Min Ko, Dohyun Han, Jong-Hee Chae, and Chul-Hwan Lee

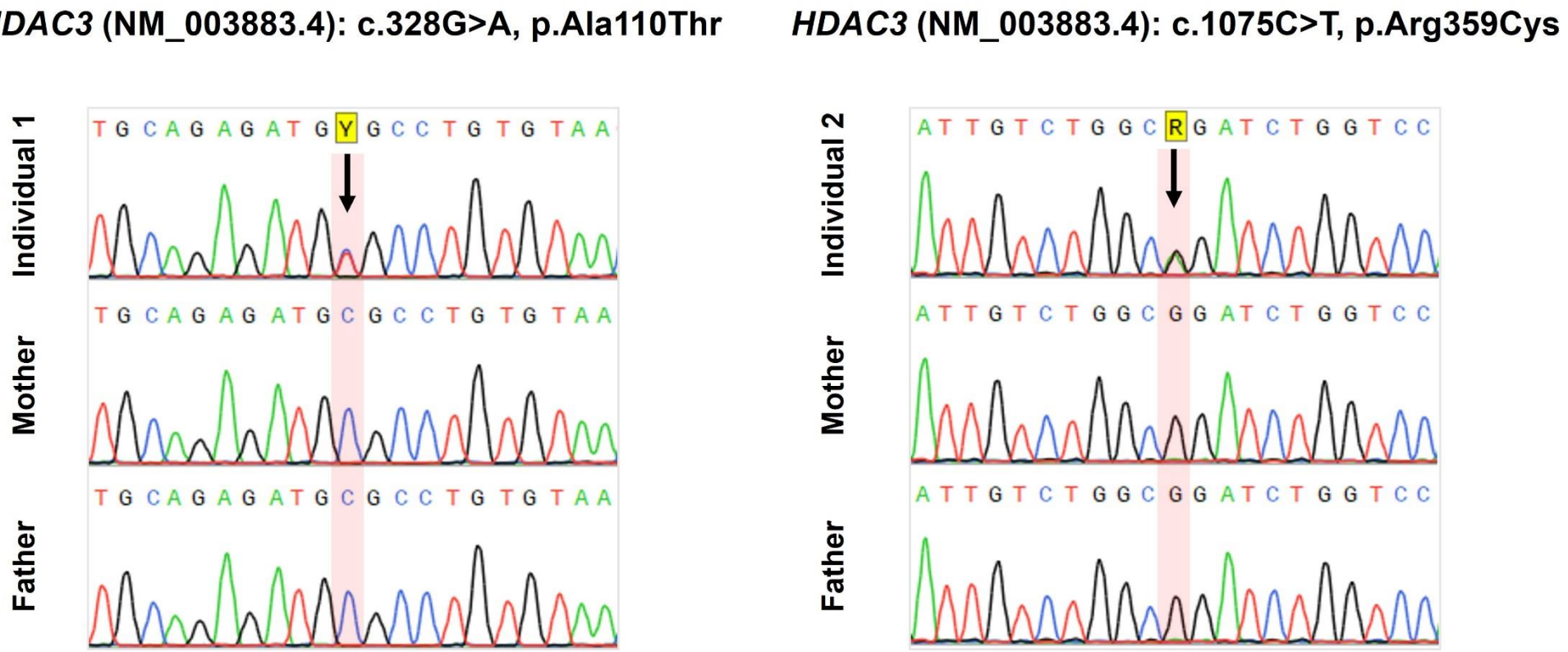

Figure S1. Confirmation of *de novo HDAC3* variants using DNA Sanger sequencing.

Sanger sequencing was conducted to validate the *de novo* variants using the primers (Table S2) for individuals 1, 2 and their parents.

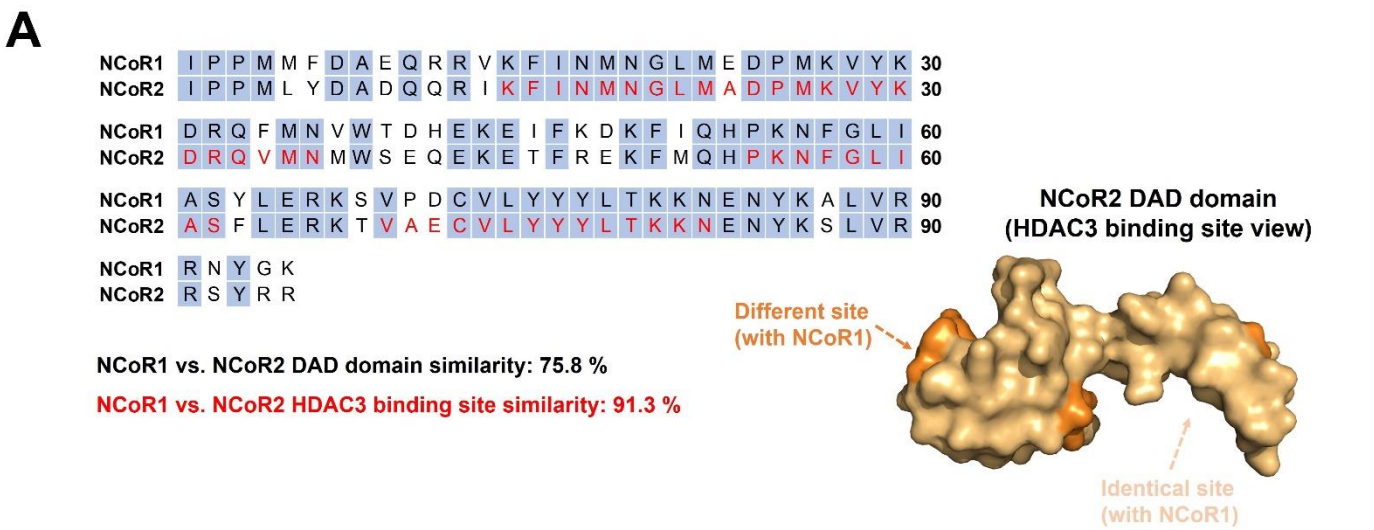

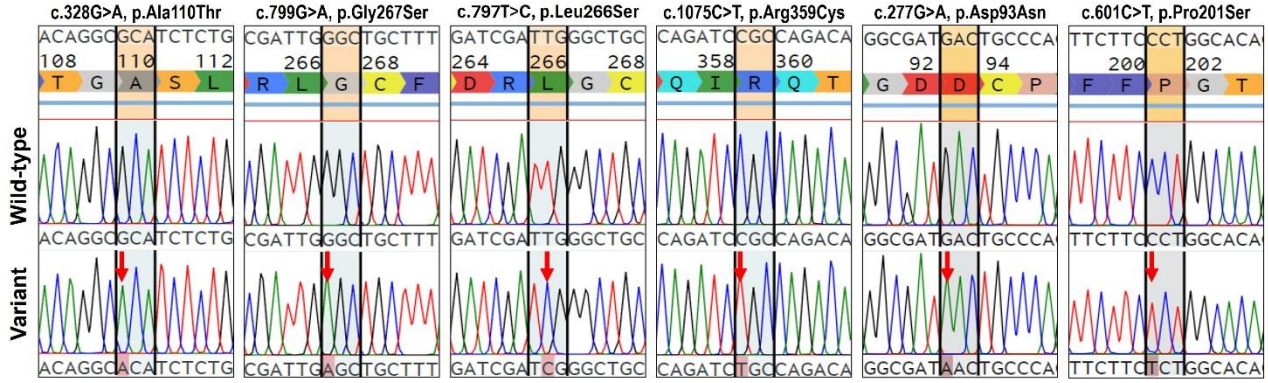

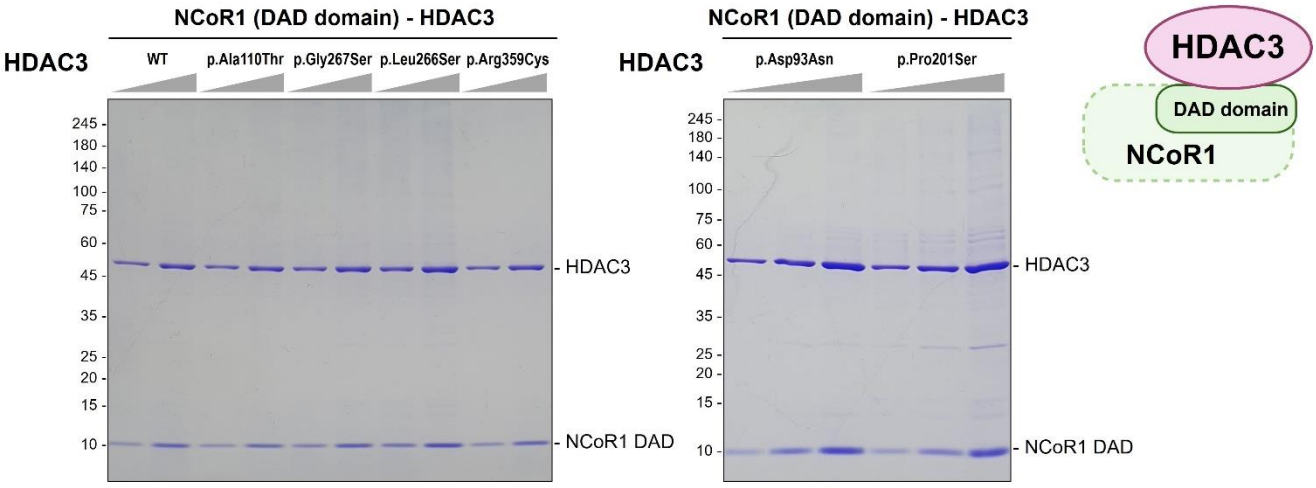

Figure S2. Characterization of NCoR1 DAD domain-HDAC3 interaction and HDAC3 mutagenesis.

(A) Sequence alignment of NCoR1 and NCoR2 DAD (Deacetylase Activating Domain) domains. This illustrates a 75.8% sequence similarity and a 91.3% similarity at the HDAC3 binding site. Alignment was conducted using the UniProt Align tool. (B) Mutagenesis of HDAC3. Six specific HDAC3 variants were introduced by PCR, utilizing mutagenic primers listed in Table S2. Sanger sequencing confirmed the presence of p.Ala110Thr, p.Gly267Ser, p.Leu266Ser, p.Arg359Cys, p.Asp93Asn, and p.Pro201Ser variants, indicating successful site-directed mutagenesis. (C) Purification of the NCoR1 DAD domain in complex with HDAC3 WT or variant proteins. These proteins, along with the NCoR1 DAD domain, were co-accumulated in Sf9 cells using a baculovirus system. Complexes were purified using Ni-NTA Agarose and Anti-FLAG M2 Affinity Gel 64hrs post-infection, as visualized on the SDS-PAGE gel, indicating no defects in their interaction with the NCoR1 DAD domain.

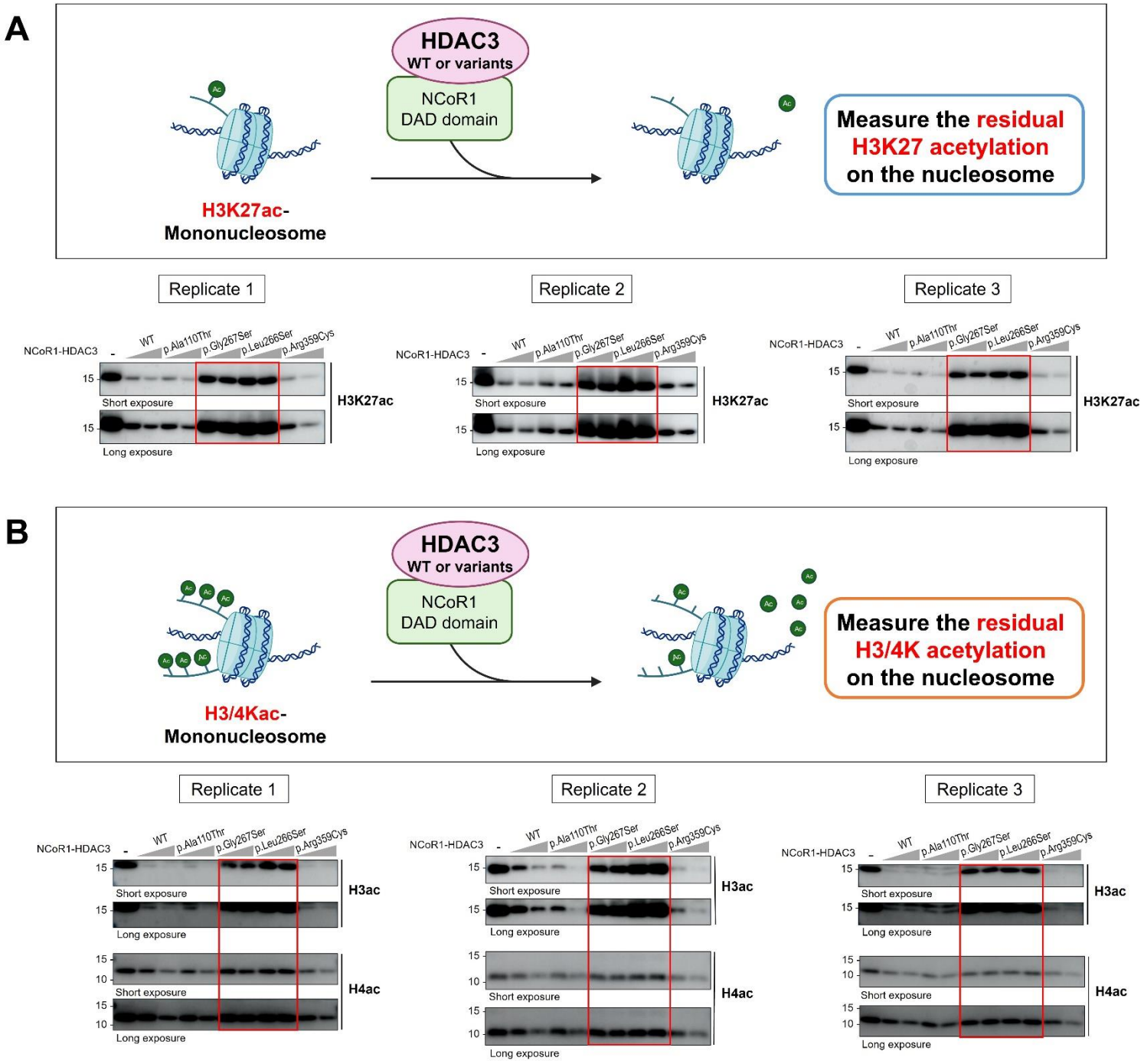
A
HDAC3
WT or variants
NCoR1
DAD domain
H3K27ac-
Mononucleosome
Measure the residual
H3K27 acetylation
on the nucleosome
Replicate 1
Replicate 2
Replicate 3
NCoR1-HDAC3
-
WT
p.Ala110Thr
p.Gly267Ser
p.Leu266Ser
p.Arg359Cys
15
Short exposure
Long exposure
H3K27ac
B
HDAC3
WT or variants
NCoR1
DAD domain
H3/4Kac-
Mononucleosome
Measure the residual
H3/4K acetylation
on the nucleosome
Replicate 1
Replicate 2
Replicate 3
H3ac
H4ac
10

Figure S3. Histone deacetylase activity of HDAC3-NCoR1 DAD domain complex on acetylated mononucleosomes.

(A) HDAC assay on H3K27ac mononucleosomes. This assay investigated the deacetylase activity of the NCoR1 DAD domain in complex with wild-type (WT) HDAC3 and its variants (p.Ala110Thr, p.Gly267Ser, p.Leu266Ser, and p.Arg359Cys). Mononucleosomes acetylated at lysine 27 on histone H3 (H3K27ac) served as substrates. Immunoblotting with an H3K27ac-specific antibody quantified the deacetylation, revealing decreased activities in the p.Gly267Ser and p.Leu266Ser variants as denoted by the red boxes. (B) HDAC assay on H3ac/H4ac mononucleosomes. This panel assesses the deacetylase activities of the NCoR1 DAD domain-HDAC3 complex, both WT and variant forms, on mononucleosomes with acetylations at various lysine residues on histones H3 (H3K4,9,14,18ac) and H4 (H4K5,8,12,16ac). Antibodies specific to acetylated H3 (H3ac) and H4 (H4ac) detected the HDAC activities. The p.Gly267Ser and p.Leu266Ser variants exhibit notably reduced deacetylase activity, as highlighted in the red boxes across all replicates.

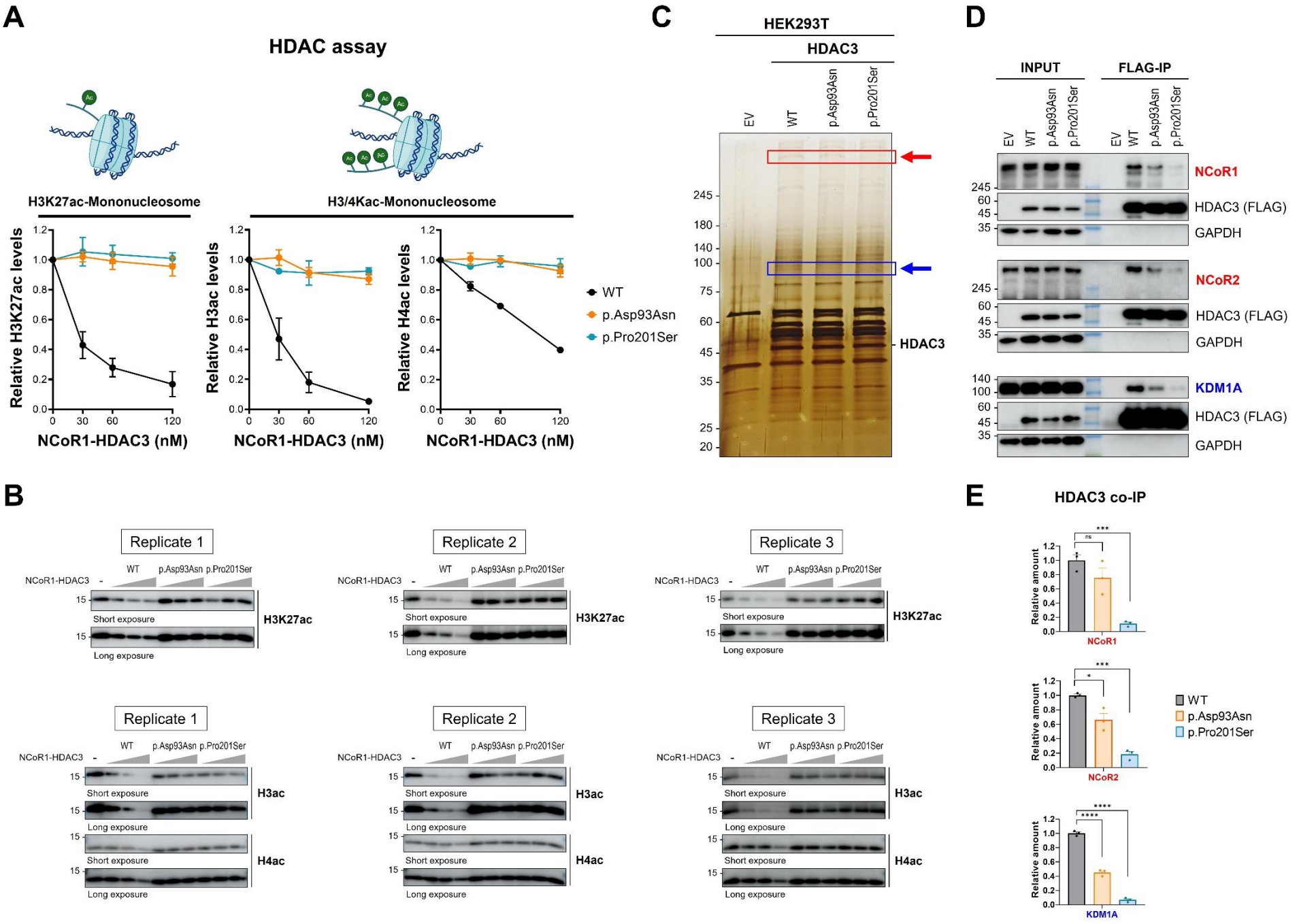
A
HDAC assay
H3K27ac-Mononucleosome
H3/4Kac-Mononucleosome
Relative H3K27ac levels
Relative H3ac levels
Relative H4ac levels
NCoR1-HDAC3 (nM)
WT
p.Asp93Asn
p.Pro201Ser
B
Replicate 1
Replicate 2
Replicate 3
NCoR1-HDAC3
WT
p.Asp93Asn
p.Pro201Ser
Short exposure
Long exposure
H3K27ac
H3ac
H4ac
C
HEK293T
HDAC3
EV
WT
p.Asp93Asn
p.Pro201Ser
HDAC3
D
INPUT
FLAG-IP
NCoR1
NCoR2
KDM1A
HDAC3 (FLAG)
GAPDH
E
HDAC3 co-IP
Relative amount
NCoR1
NCoR2
KDM1A
WT
p.Asp93Asn
p.Pro201Ser

Figure S4. Defective HDAC activity and decreased interactions with NCoR1/2 and KDM1A in *HDAC3* p.Asp93Asn and p.Pro201Ser variants.

(A) HDAC assays were conducted using H3K27ac-mononucleosomes or H3/4Kac-mononucleosomes as substrates at various concentrations (0, 30, 60, 120 nM), in conjunction with 100 nM of acetylated mononucleosomes. The deacetylation activities of complexes comprising either the NCoR1 DAD domain-HDAC3 WT or variant forms were measured for histone H3K27ac, H3ac, and H4ac in triplicate (*n*=3/data point). The results are plotted as mean ± SD. The p.Asp93Asn and p.Pro201Ser variants do not result in histone acetylation levels comparable to the WT, indicating defective HDAC activity. (B) Western blot images for HDAC activity assessment using the HDAC3-NCoR1 DAD domain complex are provided. The analysis was performed in triplicate, with both short and long exposures displayed. (C) Silver-stained SDS-PAGE analysis demonstrating the protein complexes co-immunoprecipitated (IP) with FLAG-tagged HDAC3 from HEK293T cells. Tested conditions include an empty vector (EV), wild-type (WT), and HDAC3 p.Asp93Asn and p.Pro201Ser variants. The band intensities corresponding to the NCoR complex (red arrow) and KDM1A (blue arrow) are reduced in the variant forms. Specifically, the p.Pro201Ser variant shows a remarkable decrease in the NCoR complex band intensity (red rectangle), and all variants exhibit diminished KDM1A bands (second band in blue rectangle). (D) Western blot analyses confirm the differential co-immunoprecipitation of NCoR1, NCoR2, and KDM1A with HDAC3 variants, using an anti-FLAG antibody for immunoprecipitation. FLAG-tagged HDAC3 and GAPDH serve as a reference for protein expression and loading control, respectively. (E) Quantification of co-immunoprecipitated NCoR1, NCoR2, and KDM1A, normalized to WT HDAC3 levels, based on the Western blot data in Panel B. **P* < 0.05, ****P* < 0.001, *****P* < 0.0001. Data are plotted as mean ± SD (*n*=3/data point).

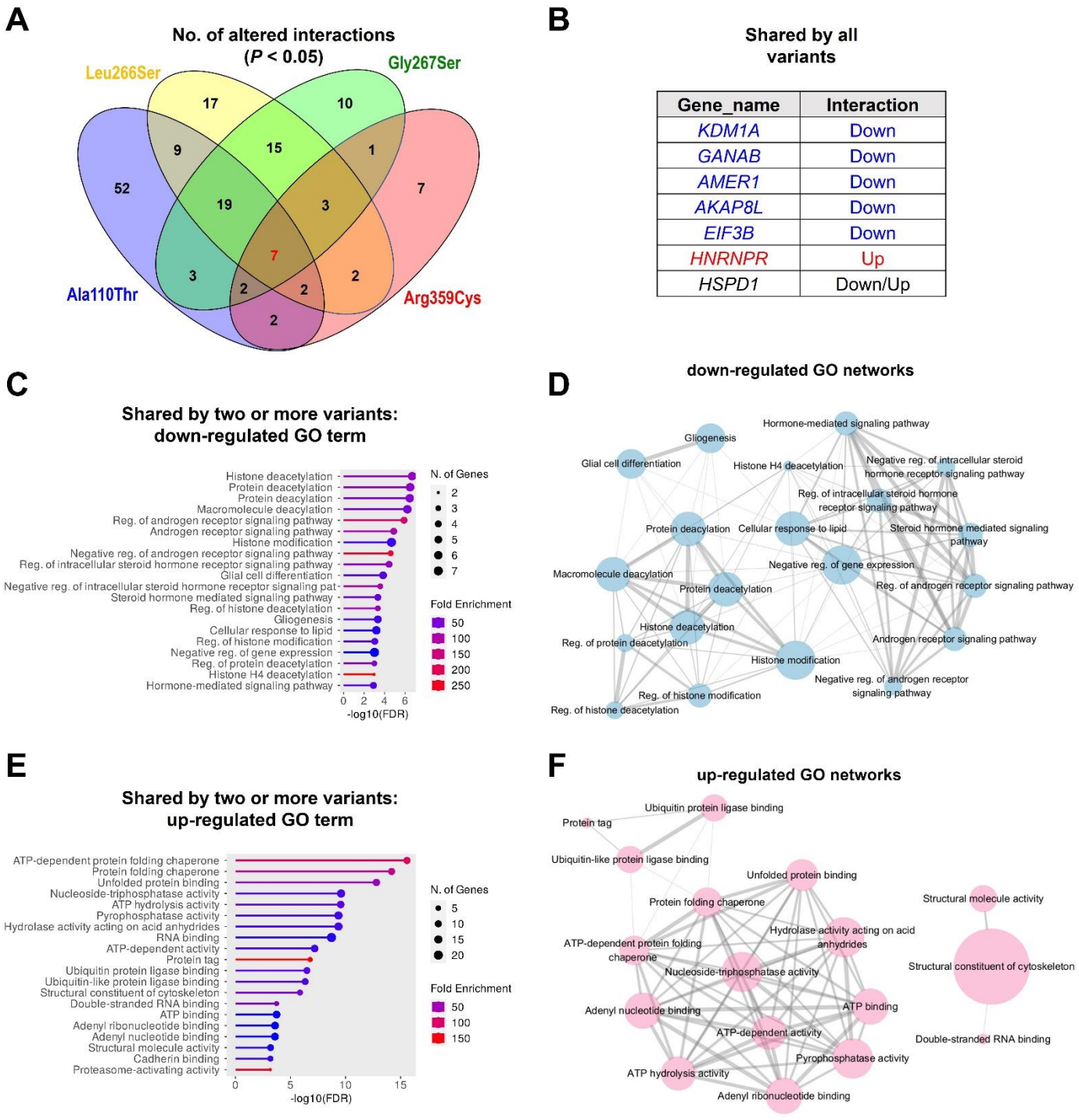

Gene_name	Interaction
KDM1A	Down
GANAB	Down
AMER1	Down
AKAP8L	Down
EIF3B	Down
HNRNPR	Up
HSPD1	Down/Up

Figure S5. Differential protein interaction profiles of HDAC3 variants in HEK293T cells.

(A) Venn diagram analysis. This panel presents a Venn diagram that quantifies the number of proteins exhibiting significantly altered interactions ($P < 0.05$) with each of four *HDAC3* variants (p.Ala110Thr, p.Leu266Ser, p.Gly267Ser, and p.Arg359Cys) in comparison to the wild-type (WT) HDAC3 in HEK293T cells. (B) Consistent interaction changes across the *HDAC3* variants. This table enumerates specific proteins that display consistent changes in interaction levels across all *HDAC3* variants tested. The proteins KDM1A, GANAB, AMER1, AKAP8L, and EIF3B show uniformly reduced interactions across the variants, indicating a possible common pathway or functional disruption. In contrast, HNRNPR, which is associated with proteasome degradation pathways, exhibits an increased interaction. (C). Pathway analysis for down-regulated GO terms. Bar chart of Gene Ontology (GO) terms enriched among proteins with decreased interaction with at least two variants, indicating decreased histone deacetylation processes (GO:0016575). (D) Network of down-regulated GO terms. A network diagram of the down-regulated GO terms connected with biological processes, revealing potential pathways impacted by the altered protein interactions. (E) Pathway analysis for up-regulated GO terms among proteins with increased interaction with at least two variants. The increased interaction with ATP-dependent protein folding chaperone (GO:0016575) molecules indicated increased protein degradation. (F) Network of up-regulated GO terms. A network diagram displaying the interconnected GO terms and molecular functions that are up-regulated, providing insight into the potential compensatory mechanisms or effects of the variant interactions.

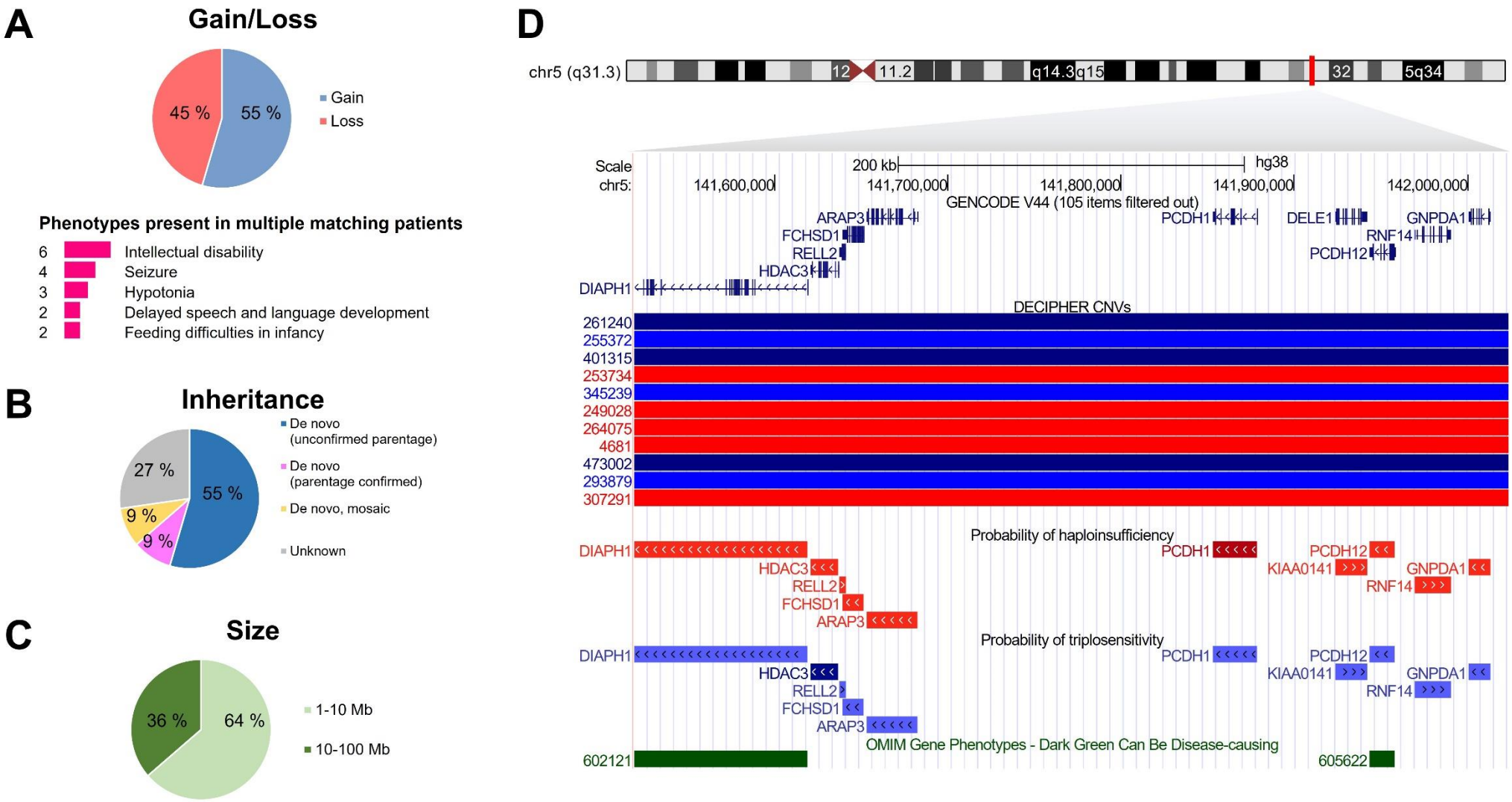
A
Gain/Loss
45 %
55 %
Gain
Loss
Phenotypes present in multiple matching patients
6 Intellectual disability
4 Seizure
3 Hypotonia
2 Delayed speech and language development
2 Feeding difficulties in infancy
B
Inheritance
27 %
55 %
9 %
9 %
De novo (unconfirmed parentage)
De novo (parentage confirmed)
De novo, mosaic
Unknown
C
Size
36 %
64 %
1-10 Mb
10-100 Mb
D
chr5 (q31.3)
12
11.2
q14.3q15
32
5q34
Scale
chr5:
200 kb
hg38
141,600,000
141,700,000
141,800,000
141,900,000
142,000,000
GENCODE V44 (105 items filtered out)
ARAP3
PCDH1
DELE1
GNPDA1
FCHSD1
RNF14
RELL2
PCDH12
HDAC3
DIAPH1
DECIPHER CNVs
261240
255372
401315
253734
345239
249028
264075
4681
473002
293879
307291
Probability of haploinsufficiency
DIAPH1
PCDH1
PCDH12
HDAC3
KIAA0141
GNPDA1
RELL2
RNF14
FCHSD1
ARAP3
Probability of triplosensitivity
DIAPH1
PCDH1
PCDH12
HDAC3
KIAA0141
GNPDA1
RELL2
RNF14
FCHSD1
ARAP3
OMIM Gene Phenotypes - Dark Green Can Be Disease-causing
602121
605622

Figure S6. Copy-number variations (CNVs) involving *HDAC3* from the DECIPHER database.

(A) CNV deletions (loss) and duplications (gain) encompassing *HDAC3*. Intellectual disability and seizure were the most prevalent phenotypes reported among the eleven patients (see Table S6). (B) Pie chart depicting the inheritance patterns of *HDAC3* CNVs, predominantly occurring *de novo*. (C) The size distribution of the CNVs. (D) The overlapping regions (chr5:141518803-142023518, 504Kb) encompassing *HDAC3* across 11 patients, as cataloged in the DECIPHER database. This region included ten genes, with *DIAPH1* and *PCDH12* identified as morbid OMIM genes (indicated in dark green). *DIAPH1* is associated with 'Deafness, autosomal dominant 1, with or without thrombocytopenia, autosomal dominant (MIM: 124900)', and 'Seizures, cortical blindness, microcephaly syndrome, autosomal recessive (MIM: 616632)', while *PCDH12* is linked to 'Diencephalic-mesencephalic junction dysplasia syndrome 1, autosomal recessive (MIM: 251280)'. The probability of haploinsufficiency (pHaplo) and triplosensitivity (pTriplo) scores for *HDAC3* are 0.62 and 1.00, respectively, ranking as the third and the highest among the genes within this region. This finding highlights *HDAC3*'s significant role in these CNVs, while also acknowledging the potential impact of gene dosage for the other genes present.

Table S1. Overview of *HDAC3* variants and *in silico* predictions.

Proband	Individual 1	Individual 2	Individual 3	Individual 4	Individual 5	Individual 6
Cohort	SNUH	SNUH	DDD	DDD	DDD	BCH
mRNA (NM_003883.4)	c.328G>A	c.1075C>T	c.277G>A	c.797T>C	c.799G>A	c.601C>T
Protein (NP_003874.2)	p.(Ala110Thr)	p.(Arg359Cys)	p.(Asp93Asn)	p.(Leu266Ser)	p.(Gly267Ser)	p.(Pro201Ser)
Origin	*De novo*	*De novo*	*De novo*	*De novo*	*De novo*	*De novo*
CADD score	27.3	32	27.3	29.9	27.5	28.3
REVEL score	0.754	0.636	0.798	0.877	0.801	0.891
DANN score	0.9993	0.9991	0.9987	0.9985	0.9989	0.9989
GERP score	4.45	5.38	5.38	5.37	5.37	5.45
PhyloP100way	7.722	6.172	7.792	9.325	7.905	10.003
ACMG/AMP classification	Likely pathogenic (PS2, PM2, PP3)	Likely pathogenic (PS2, PP2, PP3)	Likely pathogenic (PS2, PM1, PM2, PP3)	Likely pathogenic (PS2, PM1, PM2, PP3)	Likely pathogenic (PS2, PM1, PM2, PP3)	Likely pathogenic (PS2, PM1, PM2, PP3)
Location on 3D structure	Close to NCoR binding domain	NLS domain, protein stability	Close to the enzymatic active site	Close to the enzymatic active site	Close to the enzymatic active site	Close to the enzymatic active site

Abbreviations: SNUH, Seoul National University Hospital; DDD, Deciphering Developmental Delay; BCH, Boston Children's Hospital; CADD, Combined Annotation Dependent Depletion[1]; REVEL, Rare Exome Variant Ensemble Learner[2]; DANN, Deleterious Annotation of genetic variants using Neural Networks[3]; GERP, Genomic Evolutionary Rate Profiling[4]; PhyloP, phylogenetic p-values[5]; ACMG/AMP, the American College of Medical Genetics and Genomics and the Association for Molecular Pathology; NLS, nuclear localization signal; IP4, inositol phosphate 4.

Table S2. Primer information.

Target	Primer	Sequences (5' to 3')[a]	Target size	T_m
HDAC3 (NM_003883.4): c.328G>A, p.Ala110Thr	Exon4_F	CCTAAGTCACAGTCCTTCCTGCC	287 bp	63.5
	Exon4_R	ATGGAGATTGGAGGAATCTAGGATG		62.9
HDAC3 (NM_003883.4): c.1075C>T, p.Arg359Cys	Exon14_F	AGGTAAGCCAGAGGCAATTAAACT	383 bp	60.8
	Exon14_R	CTGAACTAGAGGTACCACTGAGATG		58.6
p.Ala110Thr mutagenesis	A110T_F	CTCTTTGAGTTCTGCTCGCGTTACACAGGCACATCTCTGCAAGGAGCAACCCAGCTGAACAAC	-	76.8
	A110T_R	GTTGTTCAGCTGGGTTGCTCCTTGCAGAGATGTGCCTGTGTAACGCGAGCAGAACTCAAAGAG		76.8
p.Gly267Ser mutagenesis	G267S_F	TGTGGAGCTGACTCTCTGGGCTGTGATCGATTGAGCTGCTTTAACCTCAGCATCCGAGGGCATGGG	-	80.4
	G267S_R	CCCATGCCCTCGGATGCTGAGGTTAAAGCAGCTCAATCGATCACAGCCCAGAGAGTCAGCTCCACA		80.4
p.Leu266Ser mutagenesis	L266S_F	TGTGGAGCTGACTCTCTGGGCTGTGATCGATCGGGCTGCTTTAACCTCAGCATCCGAGGGCATGGG	-	82.3
	L266S_R	CCCATGCCCTCGGATGCTGAGGTTAAAGCAGCCCGATCGATCACAGCCCAGAGAGTCAGCTCCACA		82.3
p.Arg359Cys mutagenesis	R359C_F	CAGAACTCACGCCAGTATCTGGACCAGATCTGCCAGACAATCTTTGAAAACCTGAAGATGCTG	-	74.8
	R359C_R	CAGCATCTTCAGGTTTTCAAAGATTGTCTGGCAGATCTGGTCCAGATACTGGCGTGAGTTCTG		74.8
p.Asp93Asn mutagenesis	D93N_F	AAGAGTCTTAATGCCTTCAACGTAGGCGATAACTGCCCAGTGTTTCCCGGGCTCTTTGAGT	-	76
	D93N_R	ACTCAAAGAGCCCGGGAAACACTGGGCAGTTATCGCCTACGTTGAAGGCATTAAGACTCTT		76
p.Pro201Ser mutagenesis	P201S_F	TCCTTCCACAAATACGGAAATTACTTCTTCTCTGGCACAGGTGACATGTATGAAGTCGGGG	-	74.2
	P201S_R	CCCCGACTTCATACATGTCACCTGTGCCAGAGAAGAAGTAATTTCCGTATTTGTGGAAGGA		74.2

[a]Mutated nucleotide sites are highlighted in red for mutagenic primers.

Table S3. List of antibodies used in this study.

Category	Name	Source	Cat No.
Primary antibody			
	FLAG M2	Sigma-Aldrich	F1804
	GAPDH	GeneTex	GTX627408
	HDAC3	Cell Signaling Technology	85057
	NCoR1	Cell Signaling Technology	5948
	NCoR2/SMRT	Cell Signaling Technology	62370
	KDM1A/LSD1	Cell Signaling Technology	2184
	β-tubulin	Abbkine	A01030
	H3K9ac	Cell Signaling Technology	9649
	H3K27ac	Abcam	ab4729
	H3ac	Active Motif	39139
	H4ac	Active Motif	39243
	H3	Abcam	ab1791
	H4	Abcam	ab10158
Secondary antibody			
	Goat anti-mouse IgG F(ab'), polyclonal antibody (HRP conjugate)	Enzo Life Science	ADI-SAB-100-J
	Goat anti-rabbit IgG, polyclonal antibody (HRP conjugate)	Enzo Life Science	ADI-SAB-300-J
	Anti-mouse IgG-Alexa Fluor 488 secondary antibody	Invitrogen	A-11001

Table S4. Quantified protein levels measured as iBAQ intensities.

Excel spreadsheets are provided for this table.

Table S5. Functional assessment results of *HDAC3* variants.

HDAC3 variants	p.Asp93Asn	p.Ala110Thr	p.Pro201Ser	p.Leu266Ser	p.Gly267Ser	p.Tyr298Cys	p.Arg301Gln	p.Arg359Cys
Location on 3D structure	Close to the enzymatic active site	Close to NCoR binding domain	Close to the enzymatic active site	Close to the enzymatic active site	Close to the enzymatic active site	Close to the enzymatic active site	NCoR/IP4 binding domain	NLS domain
HDAC activity[b]	Impaired	Unaffected	Impaired	Impaired	Impaired	Impaired (predicted)[a]	Impaired (predicted)[a]	Unaffected
NCoR complex integrity[c]	Impaired	Impaired	Impaired	Impaired	Impaired	Impaired (predicted)[a]	Impaired (predicted)[a]	Unaffected
CoREST complex integrity[c]	Impaired	Impaired	Impaired	Impaired	Impaired	Impaired (predicted)[a]	Impaired (predicted)[a]	Impaired
Nuclear localization[d]	Not tested	Decreased	Not tested	Decreased	No significant changes	Not tested	Not tested	Mildly decreased

[a]Predicted impairment based on structural proximity to critical domains, and previous functional experiments.[6,7] [b]see Figures 2, S4A for the relevant findings. [c]see Figures 3, 4, S4B, S4C, S4D for the relevant findings. [d]see Figure 5 for the relevant findings.

Abbreviations: HDAC, histone deacetylase; NCoR, nuclear receptor co-repressor; IP4, inositol phosphate 4; CoREST, co-repressor of repressor element 1 silencing transcription factor; NLS, nuclear localization signal;

Table S6. The complete list of patients involving *HDAC3* in the DECIPHER database.

Patient	Sex	Location (hg38)	Size (Mb)	Type	Numbers of genes	Inheritance / Genotype	Phenotypes
4681	46XX	5:139757679-142322798	2.57	Deletion	110	Heterozygous *de novo* (unconfirmed parentage)	Delayed speech and language development; Feeding difficulties in infancy; Hypotonia; Intellectual disability; Seizure
307291	46XX	5:141518803-144474238	2.96	Deletion	30	Heterozygous *de novo* (parentage confirmed)	Camptodactyly of finger; Eczema; Flexion contracture of toe; Hypohidrosis
253734	46XY	5:138175200-143214961	5.04	Deletion	162	Heterozygous *de novo* (unconfirmed parentage)	Feeding difficulties in infancy; Hypotonia; Intellectual disability
264075	46XX	5:139221860-145752584	6.53	Deletion	155	Heterozygous *de novo* (unconfirmed parentage)	Abnormal plantar dermatoglyphics; Broad face; Lissencephaly; Seizure
249028	46XX	5:138871137-145812309	6.94	Deletion	160	Heterozygous *de novo* (unconfirmed parentage)	Abnormality of the upper respiratory tract; Coarse facial features; Hypotonia; Intellectual disability; Patent ductus arteriosus
293879	46XX	5:140963199-142023518	1.06	Duplication	74	Heterozygous (unknown)	Not available
401315	46XX	5:134611071-143666887	9.06	Duplication	224	Heterozygous *de novo* (unconfirmed parentage)	Abnormal pinna morphology; Brachycephaly; Constipation; Deeply set eye; Delayed speech and language development; Diabetes mellitus; EEG abnormality; Fine hair; Gait disturbance; Hypertelorism; Intellectual disability; Mandibular prognathia; Precocious puberty in females; Prominent nose; Recurrent infections; Scoliosis; Short philtrum; Strabismus; Wide mouth
345239	Unknown	5:138673406-150130520	11.46	Duplication	230	Heterozygous (unknown)	Not available
473002	46XX	5:140753223-156697007	15.94	Duplication	239	Heterozygous (unknown)	Not available
255372	46XY	5:131740228-149668223	17.93	Duplication	348	Heterozygous *de novo* (unconfirmed parentage)	2-3 toe syndactyly; Inguinal hernia; Intellectual disability; Microcephaly; Sacral dimple; Seizure; Short stature
261240	46XX	5:124516041-149272148	24.76	Duplication	384	Heterozygous *de novo* (mosaic)	Intellectual disability; Seizure

Supplemental References

1. Rentzsch P, Witten D, Cooper GM, Shendure J, Kircher M. CADD: predicting the deleteriousness of variants throughout the human genome. *Nucleic Acids Res*. 2019;47(D1):D886-D894. doi:10.1093/nar/gky1016

2. Ioannidis NM, Rothstein JH, Pejaver V, et al. REVEL: An Ensemble Method for Predicting the Pathogenicity of Rare Missense Variants. *Am J Hum Genet*. 2016;99(4):877-885. doi:10.1016/j.ajhg.2016.08.016

3. Quang D, Chen Y, Xie X. DANN: a deep learning approach for annotating the pathogenicity of genetic variants. *Bioinformatics*. 2015;31(5):761-763. doi:10.1093/bioinformatics/btu703

4. Cooper GM, Stone EA, Asimenos G, Green ED, Batzoglou S, Sidow A. Distribution and intensity of constraint in mammalian genomic sequence. *Genome Res*. 2005;15(7):901-913. doi:10.1101/gr.3577405

5. Pollard KS, Hubisz MJ, Rosenbloom KR, Siepel A. Detection of nonneutral substitution rates on mammalian phylogenies. *Genome Res*. 2010;20(1):110-121. doi:10.1101/gr.097857.109

6. Sun Z, Feng D, Fang B, et al. Deacetylase-Independent Function of HDAC3 in Transcription and Metabolism Requires Nuclear Receptor Corepressor. *Mol Cell*. 2013;52(6):769-782. doi:10.1016/j.molcel.2013.10.022

7. Lahm A, Paolini C, Pallaoro M, et al. Unraveling the hidden catalytic activity of vertebrate class IIa histone deacetylases. *Proc Natl Acad Sci USA*. 2007;104(44):17335-17340. doi:10.1073/pnas.0706487104